Multilayered Cloud Retrieval Over ARM SGP

J.-P. Huang, Y.-H. Yi, and M. M. Khaiyer
AS&M Inc.
Hampton, Virginia

P. Minnis and B. Lin
National Aeronatic Space Administration
Langley Research Center
Hampton, Viriginia

R. F. Arduini
SAIC
Hampton, Virginia

G. G. Mace
Department of Meteorology
University of Utah
Salt Lake City, Utah

Introduction

Ice water path (*IWP*) determination is often complicated because of cloud overlap. Current satellite *IWP* retrievals are usually based on the assumption that all clouds are single-layered, despite the relatively frequent occurrence of overlapped cloud systems. Although *IWP* can be inferred from retrievals of cloud optical depth and effective ice particle sizes using visible (VIS) and infrared (IR) methods (Minnis et al. 1993, 1995, 1998, 2001), it is generally overestimated when water clouds are present underneath the ice clouds. Methods for direct retrievals of ice cloud properties using millimeter and sub-millimeter-wavelength measurements in all conditions (Liu and Curry 1998, 1999; Weng and Grody 2000; Zhao and Weng 2002) are under development but have not yet been deployed on satellites. However, even for these newer techniques there are no cloud property estimates for the lower cloud layers in multi-layer systems.

Currently, the most feasible approach for retrieving *IWP* for the overlapped cases uses a combination of microwave (MW) and VIS-IR methods. Lin et al. (1996, 1998) estimated global *IWP* distributions over oceans by using a simple separation technique of total water path (*TWP*). *TWP*, which is assumed to be equal to the combination of liquid water path (*LWP*) and *IWP*, is retrieved from VIS/IR data, and cloud *LWP* is retrieved from a MW remote sensing method. Those estimates mark an advance in our knowledge of global *IWP* but they are limited to ocean areas, are based on the simple *TWP-LWP* difference technique, and are difficult to validate.

Over land, the variability in surface emissivity renders such an approach nearly useless. However, at several Atmospheric Radiation Measurement (ARM) Program (Ackerman and Stokes 2003) surface sites, *LWP* is routinely derived from MW radiometers(MWR) and, at one location, cloud vertical structure is determined accurately from a combination of cloud lidars and radars. In some cases, it is possible to simultaneously derive the *IWP* from the radar data even when *LWP* is present (Mace et al. 2002). By combining the satellite retrievals from the Geostationary Operational Environmental Satellite (GOES) with the surface-derived *LWP* over the ARM sites, it should be possible to develop a more complete *IWP* climatology over this limited region for single- and multilayered clouds and perform some validation comparisons with the surface-based IWP retrievals for multilayered clouds.

In this study, an improved technique is developed to estimate *LWP* and *IWP* values simultaneously using satellite and ground-based measurements over ARM Southern Great Plains (SGP). Rather than simply differencing the *TWP* and MW *LWP* in overlapped cases, this new approach performs a more explicit radiance-based retrieval of *IWP* to account for differences in the optical properties of ice and liquid water clouds.

Satellite and Surface Data

This study analyzes satellite and surface measurements taken between 1 March and 30 October 2000 over the ARM SGP domain. GOES-8 provided continuous coverage of the region and was used to derive the daytime cloud properties using the visible infrared solar-infrared split-window technique (VISST), which is an upgrade of the 3-channel method described by Minnis et al. (1995, 1998, and 2002). An algorithm adapted from the satellite remote sensing method of Lin et al. (1998, 2001) was used to retrieve *LWP* and liquid water temperature, *Tw,* from the ground-based ARM SGP MWR and infrared thermometer (IRT) measurements. ARM's ground-based MWRs are available at several locations within the SGP domain (Liljegren 1999; Clothiaux et al. 2000). Surface pressure and air temperature, as well as temperature and wind direction at cloud base height, were provided by Rapid Update Cycle (RUC) (Benjamin et al. 2004) 3-hourly model output. The ARM MWRs measure 23.8 and 31.4 GHz brightness temperatures at 20-second sampling intervals. Before retrieving *LWP* and *Tw*, the 2-s data were averaged over 3-minute intervals to reduce *Tb* measurement noise and facilitate processing.

The ice-over-water clouds are identified using the MVI method, which uses the difference between cloud liquid water temperature *Tw* and the effective cloud temperature *Tc.* The cloud liquid water temperature *Tw* retrieved from IRT data is close to cloud base temperature, especially when the lower level clouds are thick (Lin et al. 2001) whereas the effective cloud temperature *Tc* derived from GOES data represents the temperature near the top of the cloud for optically thick clouds (Minnis et al. 1993). When the difference, $\Delta Twc = Tw - Tc$, is significantly larger than zero, it is likely that the observed system consists of overlapped or mixed phase clouds (Lin et al. 1998; Ho et al. 2003). In this study, the conditions required for classifying a cloud as ice-over-water for the entire 0.3° box is: 100% ice phase, $Tc < 273$K, $Tw\text{-}Tc > 8$ K and MWR *LWP* (LWP_{MW}) > 0.0 gm^{-2}. Multilayered clouds were detected in 60% of the total occurrences of overcast ice clouds from all four sites. Most of the overlapped cloud systems consist of cold, high ice cloud over lower, warmer water cloud (Huang et al. 2003).

Development of Multilayered Cloud Retrieval System (MCRS)

In the MVI method, it is assumed that, for overcast multilayered ice-over-water clouds, the VISST-derived *IWP* equals *TWP*. Therefore, the "true" ice water is estimated by the MVI technique through simple differencing as

$$IWP = TWP - LWP \quad (1)$$

where *LWP* is from the MWR retrieval. In reality, the microphysical properties of the low-level clouds significantly influence the VISST-derived optical depths and effective diameters subjecting the simple differencing method to potentially large biases.

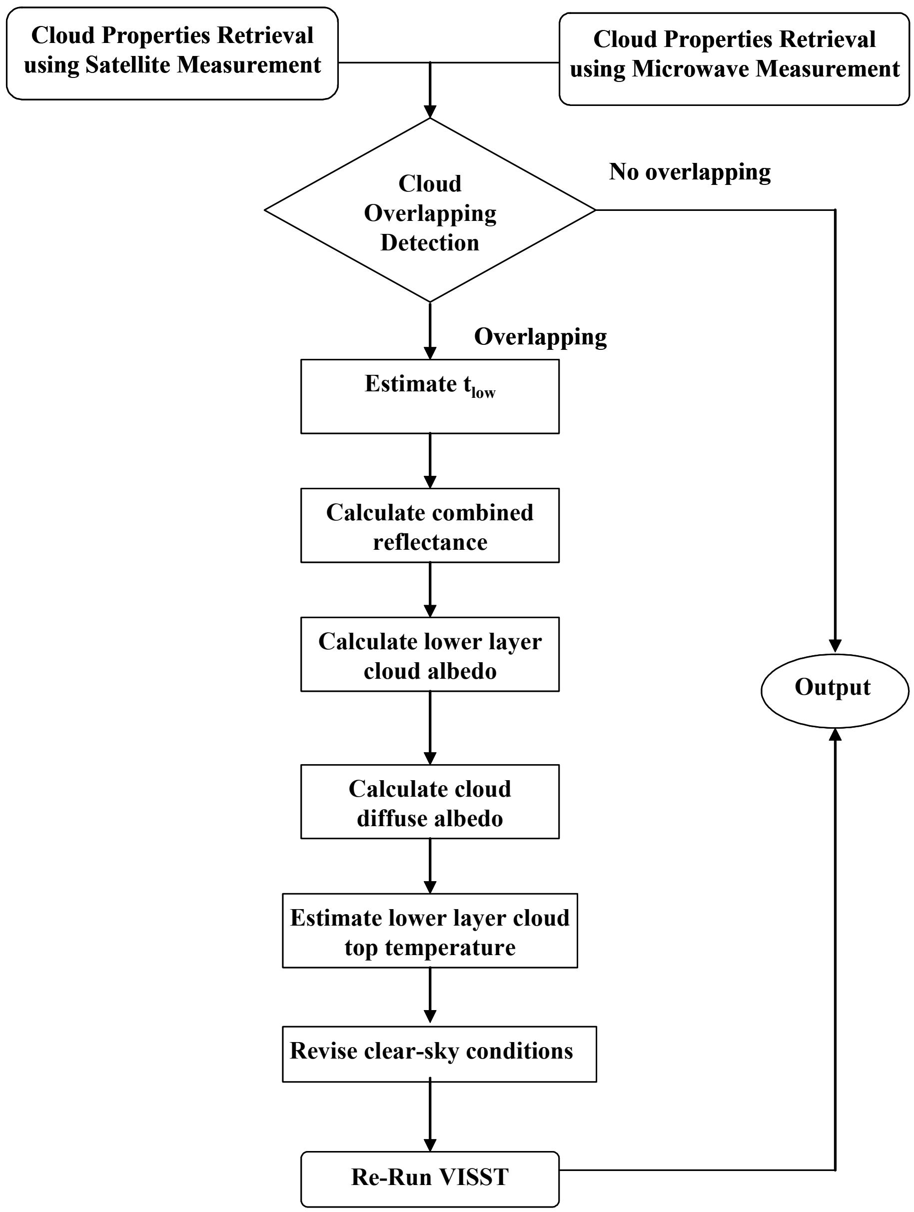

Figure 1. Schematic view of the multilayered cloud retrieval system (MCRS).

To improve the accuracy of ice cloud property retrievals, a new retrieval algorithm is developed for multilayered cloud system. A schematic view of this new algorithm, the multilayered cloud retrieval system (MCRS), is outlined in Figure 1. Initially, the VISST retrieval is performed using the surface as the background and the MWR retrieval is used to derive *LWP* and *Tw*. The results are used in the MVI method to detect the cloud overlapping by using the difference between the value of cloud water temperature *Tw* retrieved from IRT data and the cloud effective temperature *Tc* derived from satellites. When the difference, $\Delta Twc = Tw - Tc$, is significantly positive, it is likely that the observed system consists of overlapped clouds (Lin et al. 1998b; Ho et al. 2003; Huang et al. 2003). Second, the optical depth of the low-level water cloud is estimated as

$$\tau_{low} = 0.75\ Q_{vis}(r_e)\ LWP_{MW} / r_e. \tag{2}$$

where $Q_{vis}(r_e)$ is the extinction efficiency at a given effective droplet radius. In this study, r_e is assumed to be 8 µm. The value of LWP_{MW} is from the MWR retrieval. In the third step, the combined reflectance is calculated by first computing the direct and diffuse reflectance at 0.65µm for the combined surface, low water cloud, and atmosphere below the low water cloud to serve as the background reflectance field for a second VISST retrieval. Similarly, the value of *Tw* is adjusted to replace the surface skin temperature used in the initial retrieval and serves to provide the background emitted radiances at 3.9, 10.8, and 12.0 µm.

Case Studies

Figure 2 shows examples of cloud radar reflectivity signals of multilayered clouds over the SCF during 3 different days in year 2000. As shown in Figure 2, the vertical structure of the multilayered cloud is complex. For example, in Figure 2d, a high (~10.5 km), cold (232.0 K) and thick ice cloud overlaps a low (~3 km), warm (284.8 K) and thin water cloud. The initial value of *Tc* from the VISST is about 53°C less than *Tw*, which translates to a height difference of ~7.5 km. The ice cloud thins out and splits in Figures 2e-f while the water layer thickens and is joined by another one. In Figure 2f, the ice cloud effective height and temperature from VISST are ~7.5 km and 255 K, respectively, and the MWR cloud water temperature is 287K. The retrieved ice cloud height is clearly less than the real upper layer cirrus altitude. The *LWP* is ~ 61 gm^{-2}, which is almost double the value in Figure 2d. Figures 2g-h also represent thick ice-over-water cloud cases except the lower layers are generally thicker than that in Figure 2c. A more complex case is seen in Figure 2a, where the lower level clouds may be doubled layered with a broken layer at bottom. Simpler cases are seen in Figures 2b, j, and k.

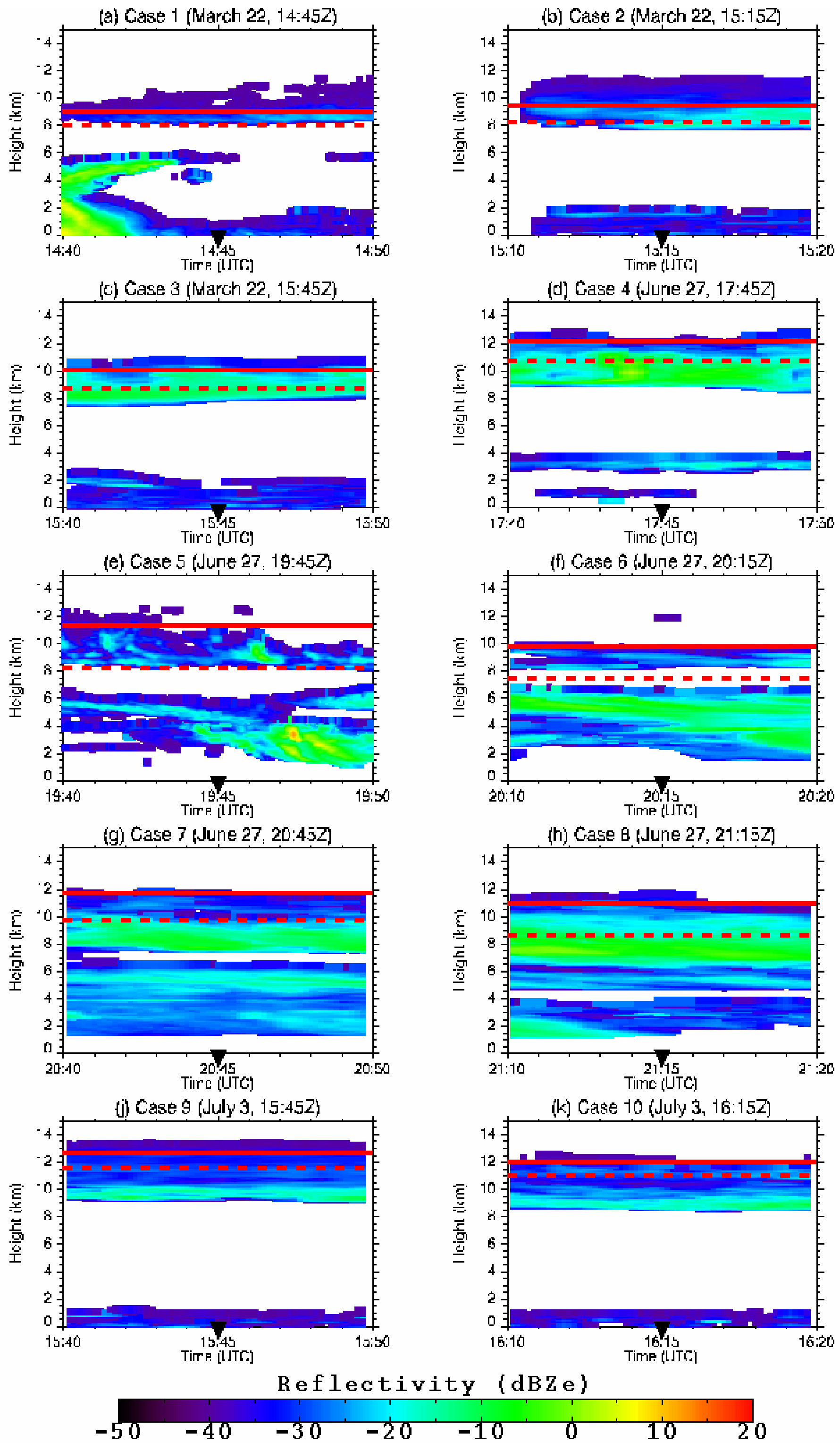

Figure 2. Millimeter Wave Cloud Radar (MMCR) reflectivity observed at ARM SGP central facility site for ten multilayered cloud cases. The solid red and dashed lines represent the cloud height derived from MCRS and VISST, respectively.

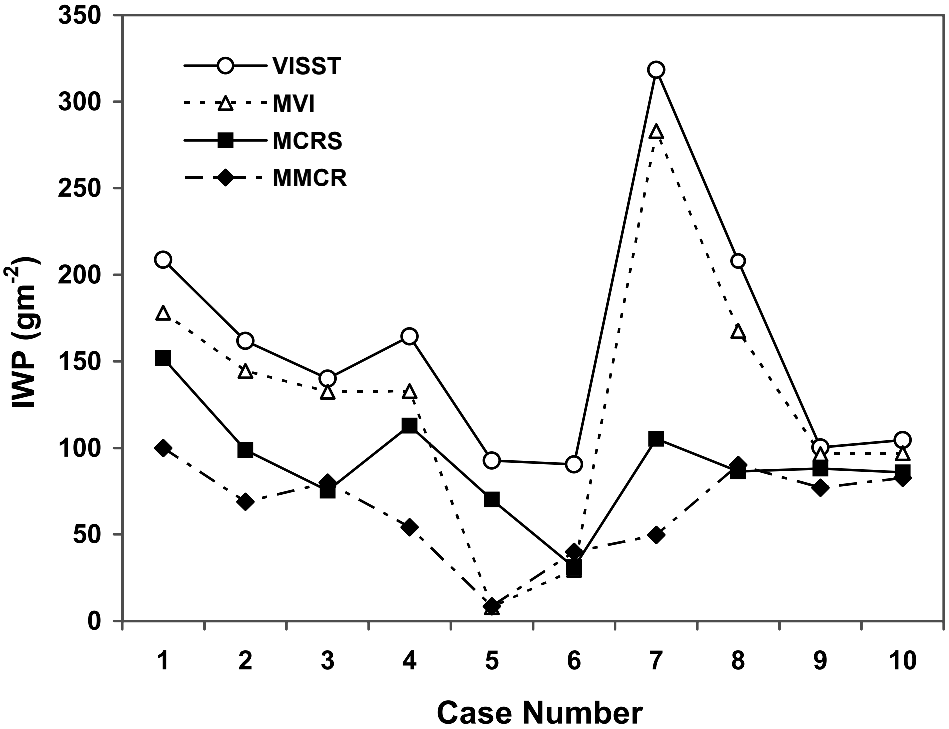

Figure 3. Comparison of *IWP* derived from the MCRS, VISST, MVI differencing (TWP-LWP), and MMCR reflectivity for the 10 cases shown in Figure 2.

Figure 3 shows a comparison of *IWP* derived from the MCRS with the values from the VISST and the MVI (see Eq. 1), and from the MMCR using an algorithm that combines measurements of Doppler velocity with radar reflectivity (Mace et al. 2002). The new MCRS algorithm produces smaller values than the VISST for all cases and the MVI for most cases. In all of the cases, except Case 5, the MCRS yields values of *IWP* that are closest to those from the radar retrieval. The differences are greatest for case 7 when *IWP* (in MCRS) is around 200 gm^{-2} less than the other two satellite retrievals. Both the MCRS and MVI results agree well with the MMCR data for Case 6, while the MVI is closest to the radar retrieval for Case 5. On average, for these cases, the difference between the MCRS and MMCR *IWP*s is 27 gm^{-2}, which is 37% of the mean MMCR value of 65 gm^{-2}. The difference is less than half that between the MVI and MMCR and almost 3.5 times smaller than the mean VISST-MMCR difference. Thus, it is clear for these results that the MCRS represents a marked improvement over both the MVI and the single-layer VISST retrieval. In both of the earlier algorithms, the *TWP* is the same. The MCRS reduces the *TWP*, on average, because it generates a new value of *IWP*. The improvement in *IWP* is consistent with the improvement of the cloud-top altitudes seen in Figure 2.

Results and Discussion

To assess how the MCRS changes the *IWP* in the multilayered overcast cases overall, it is necessary to examine all of the results from the four sites over the 8-month period. Figure 4 compares the ice cloud properties derived using the MCRS (black bar) with the VISST (gray bar) for ice-over-water cloud systems. The major differences between the two methods are evident in the optical depth frequency distributions (Figure 4a). The optical depths derived from the MCRS are significantly shifted to smaller values. Cloudy pixels with $\tau < 8$ comprise more than 30% of the data compared to only 9% for the VISST retrievals. The 8-month mean optical depth drops to 29.7 from 38.6. The mean relative change in τ is around 30.5% given that the relative change is defined as

$$R_c(X_{MCRS}) = \frac{(X_{VISST} - X_{MCRS})}{X_{VISST}} * 100\% \tag{3}$$

where X_{VISST} and X_{MCRS} are the cloud properties derived from VISST and MCRS, respectively. For *De*, the March-October mean from this study (Figure 4b) is 64.9 µm, which is 1.3 µm greater than the original VISST average *De*. The averaged relative change is ~3.79%. As expected, the ice water path (*IWP)* values derived from current algorithm (Figure 4c) are considerably smaller than those derived from VISST; the March-October mean *IWP* decreases from 844.9 gm^{-2} to 632.7 gm^{-2}. For the MCRS retrievals, clouds with $IWP < 200$ gm^{-2} account for around 40% of the total compared to only 20% of those from VISST. The mean relative change is 33.7%, which is only slightly lager than $R_c(\tau)$ but much larger than that for the ice diameter.

Figure 5 shows R_c for the three ice cloud properties as a function of VISST optical depth (τ_{VISST}) for ice-over-water clouds. The τ_{VISST} derived from the reflected visible radiance represents the combined effects of all cloud layers. As such, cloud overlap causes large errors in the retrievals of ice cloud optical depth, ice water path, and particle size. For more than 75% of the overcast overlapping clouds ($\tau_{VISST} \leq 60$, also see Figure 4a), the MCRS reduces the ice cloud optical depth and *IWP* by more than 30%. The relative change for larger optical depths is generally smaller suggesting that in those cases, the ice cloud contains most of the mass in the multilayered systems. The maximum R_c for *IWP* and τ, ~ 45%, occurs at $\tau_{VISST} = 35$. However, for multilayered clouds with $\tau_{VISST} > 60$, R_c for τ and *IWP* decreases with the increasing of τ_{VISST}. For thin overlapped clouds ($\tau_{VISST} \leq 10$), the results from the new algorithm indicate that *De* is underestimated by 15% (i.e., $R_c(De)$ ~ -15%), but $R_c(De)$ becomes very small when τ_{VISST} exceeds 10. Given that $R_c(\tau)$ averages about 30% or less for $\tau_{VISST} > 10$, it is evident that the ice clouds are generally optically thick and, therefore, the initial VISST retrieval yields a relatively accurate value of *De*. On average relative to the VISST, the MCRS reduces τ and *IWP* by 8.9 (23%) and 212.1 gm^{-2} (25%), respectively, and increases *De* by 1.3 µm (2%).

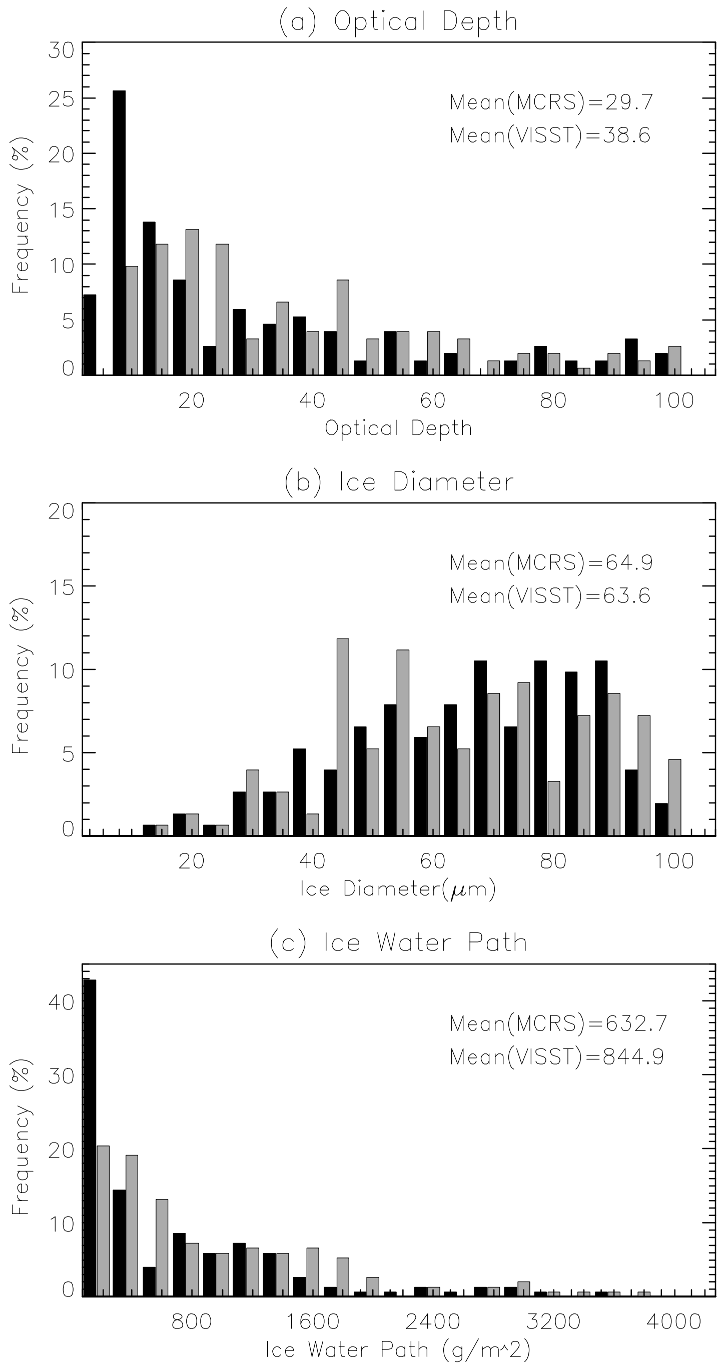

Figure 4. Comparison of ice cloud properties derived from MCRS (black bar) with VISST (gray bar) for (a) optical depth, (b) ice diameter, and (c) ice water path for ice-over-water clouds over four ARM SGP sites (March-October, 2000). The histogram bins are 5 for (a), 5 μm for (b), and 200 gm^{-2} for (c).

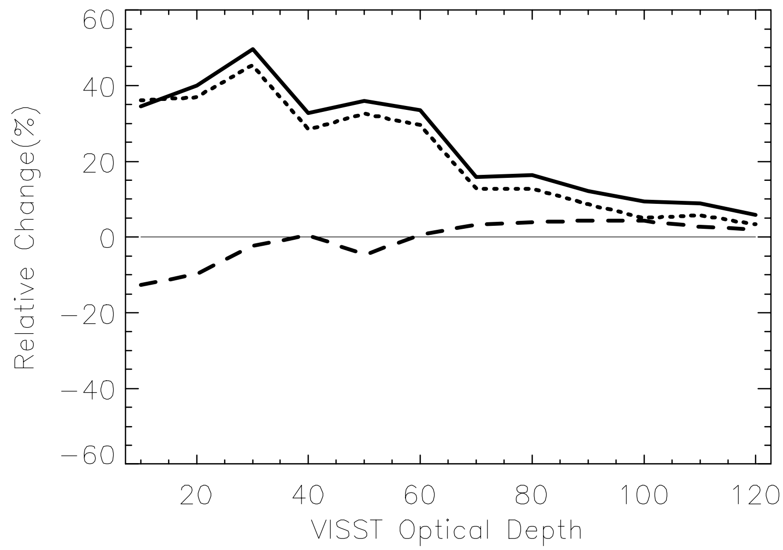

Figure 5 Relative change rates of ice cloud properties derived from MCRS to the properties derived from VISST as a function of VISST optical depth for ice-over-water clouds over four ARM SGP sites (March-October, 2000). Solid line is for IWP, dotted line for optical depth and dashed line for ice diameter.

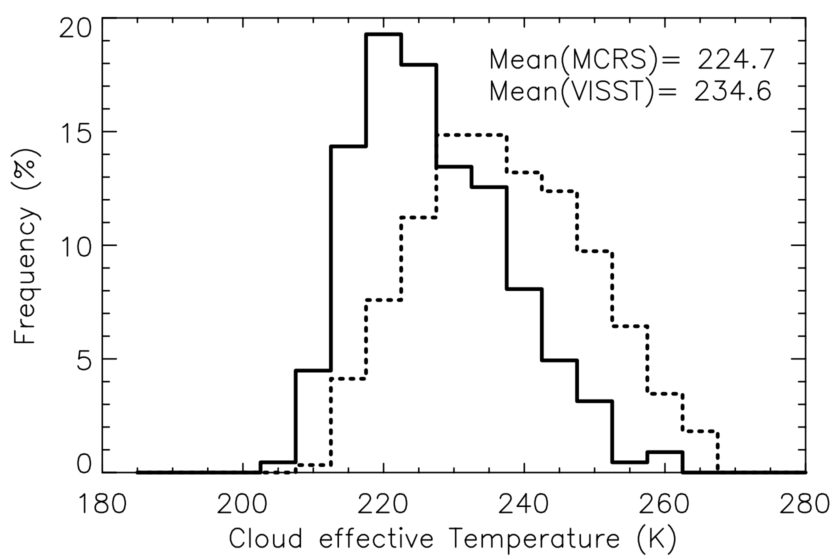

Figure 6. Comparison of cloud effective temperature derived from MCRS (solid line) and VISST (dished line) for ice-over-water cloud systems over four ARM SGP sites (March-October, 2000). The histogram bin is 5 K.

Figure 6 compares the histogram of upper layer cloud effective temperature derived from new algorithm (solid line) and VISST (dashed line). The temperatures from the new algorithms are decreased by

10 ± 12 K, on average, which translates to a height difference of ~1.4 km. The results in Figures 2 and 6 indicate that ice-cloud height derived from traditional single-layer satellite retrieval is underestimated and over classifies mid-level ice cloud coverage.

Conclusions

A more rigorous multilayered cloud retrieval system has been developed to improve the determination of high cloud properties in multilayered clouds. The MCRS attempts a more realistic interpretation of the radiance field than earlier methods because it explicitly resolves the radiative transfer that would produce the observed radiances. A two-layer cloud model was used to simulate multilayered cloud radiative characteristics. It uses a simplified visible reflectance parameterization that could produce some uncertainties that will be examined in future studies. Surely, use of explicit two-level radiative transfer calculations could reduce the uncertainties in the retrievals. Despite the use of a simplified two-layer cloud reflectance parameterization, the MCRS clearly produced a more accurate retrieval of ice water path than the simple differencing techniques used in the past. The initial results indicate that it still might be overestimating *IWP* for overlapped cases, but by much smaller amounts than other techniques. However, many more comparisons are needed with radar-MWR retrievals and a better assessment of the errors in the radar retrievals is needed. The method is not particularly sensitive to the assumed droplet size or the uncertainties in the MWR retrievals. The errors are smaller than the differences between the radar and MCRS retrievals. Thus, this new physically based technique should be robust and directly applicable when the proper microwave and imager data are available.

Acknowledgements

This research was supported by the Environmental Sciences Division of U.S. Department of Energy through the Interagency Agreements DE-AI02-97ER62341 and DE-AI02-02ER63319 under the ARM program.

Corresponding Author

J.-P. Huang, j.huang@larc.nasa.gov, (757) 827-4624

References

Ackerman, T., and G. Stokes, 2003: The Atmospheric Radiation Measurement Program, *Physics Today,* **56,** 38 – 45.

Benjamin, S. G., D. Devenyi, S. S. Weygandt, K. J. Brundage, J.M. Brown, G.A. Grell, D. Kim, B. E. Schwartz, T. G. Smirnova, T. L. Smith, and G. S. Manikin, 2004: An hourly assimilation – forecast cycle: The RUC, *Mon Wea. Rev.*, **132**, 495-518.

Clothiaux, E. E., T. P. Ackerman, G. G. Mace, K. P. Moran, R. T. Marchand, M. Miller, and B. E. Martner, 2000: Objective determination of cloud heights and radar reflectivities using a combination of active remote sensors at the ARM CART sites, *J. Appl. Meteorol.*, **39**, 645-665.

Ho, S.-P., B. Lin, P. Minnis, and T.-F. Fan, 2003: Estimation of cloud vertical structure and water amount over tropical oceans using VIRS and TMI data, *J. Geophys. Res.*, **108,** 10.1029/2002JD003298.

Huang, J.-P., M. M. Khaiyer, P. W. Heck, P. Minnis, and B. Lin, 2003: Determination of ice-water path over the ARM SGP using combined surface and satellite datasets. In *Proceedings of the Thirteenth Atmospheric Radiation Measurement (ARM) Science Team Meeting*, ARM-CONF-2003. U.S. Department of Energy, Washington, D.C. Available URL: http://www.arm.gov/publications/proceedings/conf13/extended_abs/huang-j.pdf

Liljegren, J. C., 1999: Automatic self-calibration of ARM microwave radiometers. *Microwave Radiometry and Remote Sensing of the Earth's Surface and Atmosphere*, Eds. P. Pampaloni and S. Paloscia, 433-443, VSP Press.

Lin, B., and W. B. Rossow, 1996: Seasonal variation of liquid and ice water path in non-precipitating clouds over oceans, *J. Climate*, **9,** 2890-2902.

Lin, B., P. Minnis, B. Wielicki, D. R. Doelling, R. Palikonda, D. F. Young, and T. Uttal, 1998: Estimation of water cloud properties from satellite microwave, infrared and visible measurements in oceanic environments, II: Results. *J. Geophys, Res.*, **103,** 3887-3905.

Lin, B., P. Minnis, A. Fan, J. A. Curry, and H. Gerber, 2001: Comparison of cloud liquid water paths derived from in situ and microwave radiometer data taken during the SHEBA/FIREACE, *Geophys. Res. Lett.*, **28,** 975-978.

Liu, G., and J. A. Curry, 1998: Remote sensing of ice water characteristics in tropical clouds using aircraft microwave data, *J. Appl. Meteorol.*, **37**, 337-355.

Liu, G., and J. A. Curry, 1999: Tropical ice water amount and its relations to other atmospheric hydrological parameters as inferred from satellite data, *J. Appl. Meteorol.*, **38**, 1182-1194.

Mace, G. G., A. J. Heymsfield, and M. R. Poellot, 2002: On retrieving the microphysical properties of cirrus clouds using the moments of the millimeter-wavelength Doppler spectrum, *J. Geophys. Res.*, **107**, 4815-4841.

Minnis, P., Y. Takano, and K.-N. Liou, 1993: Inference of cirrus cloud properties using satellite-observed visible and infrared radiances, Part I: Parameterization of radiance fields, *J. Atmos. Sci.*, **50**, 1279-1304.

Minnis, P., D. F. Young, D. P. Kratz, J. A. Coakley, Jr., M. D. King, D. P. Garber, P. W. Heck, S. Mayor, and R. F. Arduini, Cloud Optical Property Retrieval (Subsystem 4.3), 1995: "Clouds and the Earth's Radiant Energy System (CERES) Algorithm Theoretical Basis Document, Volume III: Cloud Optical Property Retrieval (Subsystem 4.3)", *NASA RP 1376 Vol. III*, edited by CERES Science Team, 135-176.

Minnis, P., D. P. Garber, D. F. Young, R. F. Arduini, and Y. Takano, 1998: Parameterization of reflectance and effective emittance for satellite remote sensing of cloud properties, *J. Atmos. Sci.*, **55**, 3313-3339.

Minnis, P., W. L. Smith, Jr., D. F. Young, L. Nguyen, A. D. Rapp, P. W. Heck, S. Sun-Mack, Q. Trepte, and Y. Chen, 2001: A near-real time method for deriving cloud and radiation properties from satellites for weather and climate studies, *Proc. AMS 11th Conf. Satellite Meteorology and Oceanography*, Madison, WI, Oct. 15-18, 477-480.

Minnis, P., L. Nguyen, D. R. Doelling, D. F. Young, W. F. Miller, and D. P. Kratz, 2002: Rapid calibration of operational and research meteorological satellite imagers, Part I: Evaluation of research satellite visible channels as references, *J. Atmos. Oceanic Technol.*, **19**, 1233-1249.

Weng, F, and N. C. Grody, 2000: Retrieval of ice cloud parameters using a microwave imaging radiometer, *J. Atmos. Sci.,* **57**, 1069-1081.

Zhao, L. and F. Weng, 2002: Retrieval of ice cloud parameters using the advanced microwave sounding unit, *J. Appl. Meteorol.*, **41,** 384-395.